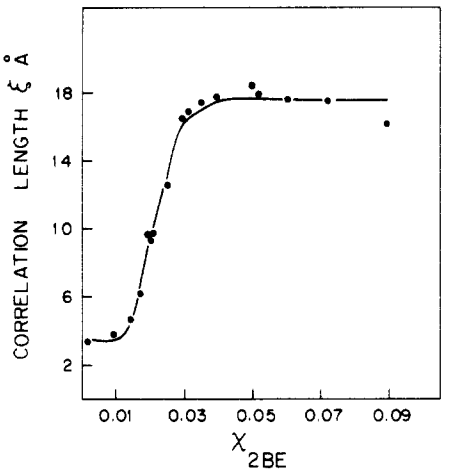

Figure 4. Correlation length of concentration fluctuations against 2BE mole fraction at 298 K. Full line is only to aid visualization.

region indicated in Figure 1 (dashed region) where bulk and surface properties display a change in their 2BE concentration dependences. In Figure 3, decreasing MDC values are a reflection of an increasing number of 2BE–water interactions in solution; however, with further increase in 2BE concentration, MDC values become constant implying that, although the concentration of 2BE is still very low, some kind of organization is present in the solution. This organization can be visualized as 2BE aggregates or pseudomicelles in solution. The MDC in Table II allows the calculation of the correlation length ξ of the concentration fluctuations in these mixtures. Assuming that velocity fluctuations are statistically independent of the concentration fluctuations,[13] ξ is related to the MDC through

$$D = \frac{kT}{6\pi\eta\xi} \tag{10}$$

Figure 4 displays ξ values calculated by using eq 10. At very low 2BE concentrations the magnitude of the correlation length (ca. 3.5 Å) is practically the same as the radius r of the 2BE molecule (3.7 Å) calculated by using the relation $(4\pi/3)r^3\rho = 1$, where ρ is the number density of 2BE. When the mole fraction of 2BE reaches ca. 0.015, ξ starts to increase rapidly; this increase is maintained over a 2BE concentration interval which, again, coincides with that indicated in Figure 1 (dashed region). An increase in 2BE concentration is not reflected on ξ which remains constant and equal to ca. 18 Å. The magnitude of this correlation length, when compared to the molecular radius, indicates considerable association of 2BE and water molecules. With further increase in 2BE concentration, ξ decreases, indicating that the interactions that held together the 2BE aggregates are fading away, and as a consequence the MDC increases.[9] It is important to point out that the large ξ values in Figure 4 occur at a temperature that is far from the lower critical solution temperature (LCST) which is located[5] at ca. 322 K and hence they cannot be assigned to the existence of this critical consolution point.

Acknowledgment. We thank J. Abarca for his technical help. This work was supported by Consejo Nacional de Ciencia y Tecnología and the Third World Academy of Sciences grants No. RGMP 88-70 and RGMP 88-67.

Registry No. 2BE, 111-76-2; W, 7732-18-5.

(13) Ferrel, R. A. *Phys. Rev. Lett.* **1970**, *24*, 1169.

Kinetics of Chemical Reactions in Condensed Media in the Framework of the Two-Dimensional Stochastic Model

M. V. Basilevsky,* V. M. Ryaboy, and N. N. Weinberg

Karpov Institute of Physical Chemistry, ul.Obukha 10, 103064 Moscow K-64, USSR
(Received: February 7, 1990; In Final Form: June 1, 1990)

A chemical reaction proceeding in a continuum medium is modeled as a pair of stochastic equations with a δ-correlated random force. A numerical method for calculating the rate constant is elaborated in a quasi-one-dimensional approximation. Exact rate constants are found over a wide range of characteristic system parameters. The existence of a significant region with a nonequilibrium kinetic behavior, as predicted previously by Berezhkovskii and Zitserman, is confirmed. Moreover, the nonequilibrium rate constant is shown to describe not only the extreme of quasi-one-dimensional dynamics but also the case when the complete two-dimensional equation of motion operates.

1. Introduction

The theory of chemical kinetics in condensed media has been successfully developed recently in terms of stochastic equations. It is not a simple matter, however, to extract kinetic information from such a treatment. The Kramers–Grote–Hynes (KGH) method[1-3] is a conventional approximation to obtain the rate constant corresponding to a generalized Langevin equation with a double-well potential. Generalizations of the KGH theory to multidimensional stochastic systems have also been reported.[4-6]

The KGH approximation is equivalent to the transition-state (TS) theory as applied to a combined system consisting of a chemical subsystem and a continuum medium.[6-9] It follows then that important dynamical effects such as nonequilibrium solvation of a chemical subsystem for reactions proceeding in highly viscous media are lacking in the KGH treatment. Such nonequilibrium phenomena can be revealed, however, if the characteristic time scales of the components in a system "a chemical subsystem + medium" are essentially different.[10,11] Therefore, one-dimensional

(1) Kramers, H. A. *Physica (Utrecht)* **1940**, *7*, 284.
(2) Grote, R. F.; Hynes, J. T. *J. Chem. Phys.* **1980**, *73*, 2715.
(3) Hanggi, P. *J. Stat. Phys.* **1986**, *42*, 105.
(4) Langer, J. S. *Ann. Phys. (N.Y.)* **1967**, *41*, 108.
(5) Weidemuller, H. A.; Zhang, J.-S. *J. Stat. Phys.* **1984**, *34*, 191.
(6) Basilevsky, M. V.; Chudinov, G. E. *Chem. Phys.*, in press.
(7) Grabert, H.; Weiss, U. *Phys. Rev. Lett.* **1984**, *53*, 1787.
(8) Pollak, E. *J. Chem. Phys.* **1986**, *85*, 865.
(9) Dakhnovskii, Yu. I.; Ovchinnikov, A. A. *Mol. Phys.* **1986**, *58*, 237.
(10) Berezhkovskii, A. M.; Zitserman, V. Yu. *Chem. Phys. Lett.* **1989**, *158*, 369.
(11) Berezhkovskii, A. M.; Zitserman, V. Yu. *Phys. A*, in press.

0022-3654/90/2094-8734$02.50/0

models like the original Kramers theory are unsuitable to study nonequilibrium solvation and related effects. The simplest potentially nonequilibrium model should explicitly involve at least two dynamical variables. The same is true in a usual (nonstochastic) dynamical theory of chemical kinetics, where in the one-dimensional case the TS method provides the exact rate expression.[12]

In the present article we consider the kinetic behavior, both equilibrium and nonequilibrium, of a simple two-dimensional model of a chemical reaction in the condensed phase. Under the condition of a large anisotropy between its intrinsic characteristic times, this system reduces to a one-dimensional one after averaging the equations of motion over the fast variable.[10,11] The resulting diffusion equation with a sink considered earlier[13,14] was studied by Sumi, Marcus, and Nadler[15,16] in the context of the electron-transfer theory. As Berezhkovskii and Zitserman showed later,[10,11] this equation generated a nonequilibrium (beyond the KGH approximation) rate constant existing in a large range of system parameters. The idea of the present work was to calculate this constant as an energy level of a quantum-mechanical Hamiltonian associated with the corresponding Liouville operator. Our calculations confirm the prediction that a single-exponential nonequilibrium kinetic regime is widespread and indicate also the existence of another nonequilibrium regime that is essentially two-dimensional and yet unknown. Along with these nonequilibrium regimes the range of parameters was determined over which equilibrium KGH kinetics works satisfactorily.

2. Description of the Two-Dimensional Model

We consider the following stochastic system as a model of a chemical reaction in a continuum media:

$$m\frac{d^2x}{dt^2} + \frac{\partial U}{\partial x} = 0$$

$$\eta\frac{dy}{dt} + \frac{\partial U}{\partial y} = \delta \text{ (correlated random force)} \qquad (1)$$

The variable x represents an internal motion in a reacting chemical subsystem with mass m (the "reaction coordinate"), whereas y is a medium coordinate. The intensity of the random force is connected with a friction coefficient η via an Einstein relation. A limitation imposed on the potential energy surface (PES) $U(x,y)$ requires that its cross section $\bar{U}(x) = U(\bar{x},y)$ at fixed $\bar{y} = y$ be double-well curves but cross sections along y at fixed x comprise single wells. So the typical potential is represented as

$$U(x,y) = U_1(x) + \tfrac{1}{2}\lambda(x)[y - y_0(x)]^2 \qquad (2)$$

Here $U_1(x)$ is a double-well curve ("the gas-phase chemical potential") whereas the medium is modeled as a harmonic oscillator with equilibrium position y_0 and force constant λ being x-dependent. The simplest version assumes $\lambda = \lambda_y$ to be constant and y_0 to be a linear function:

$$U(x,y) = U_1(x) + \tfrac{1}{2}\lambda_y[y - \alpha x]^2 \qquad (3)$$

We postulate that a Boltzmann distribution is maintained in the reactant region located around the respective PES minima. This eliminates such kinetic regimes as an energetic diffusion inherent to the one-dimensional Kramers model. However the reaction process can disturb this equilibrium distribution apart from the reaction region, which results in nonequilibrium kinetics. The potential in the vicinity of its saddle point is conventionally approximated as a paraboloid one. In the case of an overlap between the region of the equilibrium distribution and that where the quadratic approximation works, the reaction flux flows over the saddle point, and the kinetics controlled by the flux in the TS region obeys the KGH theory fairly well. In this case[5]

$$k = \frac{\Omega}{2\pi}\left(\frac{\det \hat{U}_0}{|\det \hat{U}^*|}\right)^{1/2}\exp(-\beta U^*) \qquad (4)$$

where β is the inverse temperature, U^* is the barrier height (activation energy), $\hat{U}_0$ and $\hat{U}^*$ are the matrices of force constants at the PES stationary points (the reactant minimum and the saddle point, respectively), and the decay frequency Ω is found as a positive root of the characteristic equation

$$\det(\Omega^2\hat{m} + \Omega\hat{\eta} + \hat{U}^*) = 0 \qquad (5)$$

in which $\hat{m}$ and $\hat{\eta}$ represent two-dimensional matrices of masses and friction coefficients, respectively.

When the anisotropy of characteristic time scales associated with x and y is large, the reaction flux flows outside the TS region.[10,11] Then the kinetics obey either a multiexponential or nonequilibrium single-exponential law following from the one-dimensional diffusion-type equation for the distribution function $P(y,t)$ of the slow medium variable:[10,11,15,16]

$$\frac{\partial P}{\partial t} = \left\{D\frac{\partial^2}{\partial y^2} - \frac{\beta D}{2}\left[\frac{\beta}{2}\left(\frac{dV}{dy}\right)^2 - \frac{d^2V}{dy^2}\right] - k(y)\right\}P \qquad (6)$$

$$\beta = (k_B T)^{-1}; \quad D = (\beta\eta)^{-1}$$

The function $P(y,t)$ is an auxiliary quantity, the true distribution function $\bar{P}(y,t)$ being related to it through $\bar{P}(y,t) = [g(y)]^{1/2}P(y,t)$, where $g(y)$ is the Boltzmann distribution in the effective potential for y motion $V(y)$. The potential $V(y)$ is

$$V(y) = U(\bar{x},y); \quad \bar{x} = \bar{x}(y)$$

$$\frac{\partial}{\partial x}U(x,y)|_{x=\bar{x}} = 0$$

which represents a cross section of an original two-dimensional PES along the line $x = \bar{x}(y)$ as formed by the reactant minima of double-well cross-sections along x at y = constant. The similar PES cross section along the line $x = \bar{x}^*(y)$ formed by maxima of the same double-well curves is designated as $V_1(y) = U(\bar{x}^*,y)$. Hereinafter we employ a quadratic approximation for these one-dimensional potentials:

$$V(y) = \tfrac{1}{2}\lambda y^2$$

$$V_1(y) = \tfrac{1}{2}\mu(y - y^*)^2 + U^* \qquad (7)$$

Now y^* is the value of y at the saddle point of $U(x,y)$ and U^* is defined earlier as a potential barrier height. The quantity

$$\Delta V(y) = V_1(y) - V(y) \qquad (8)$$

defines a local potential barrier for a chemical reaction proceeding at different values of the medium coordinate. Finally, the local rate constant $k(y)$ ("the sink") is defined as

$$k(y) = \frac{\omega_e}{2\pi}\exp[-\beta\Delta V(y)] \qquad (9)$$

$$\omega_e = \left(\frac{\lambda_x + \alpha^2\lambda_y}{m}\right)^{1/2}$$

where ω_e is the local frequency for the x motion at point $\bar{x}(y)$ and λ_x is the force constant of the double-well function $U_1(x)$ at this point. Generally speaking, λ_x depends on y and so does ω_e. This dependence seems to be of secondary importance and will be neglected in the subsequent treatment. Thereby some limitation is imposed on $U_1(x)$, namely, λ_x should be considered as constant within a finite x interval around its minimum. The explicit potential exactly representing this property and obeying conditions 7 is considered in Appendix A.

(12) Pechukas, P. In *Dynamics of Molecular Collisions, Part B*; Miller, W. H., Ed.; Plenum: New York, 1976; p 269.
(13) Agmon, N.; Hopfield, J. I. *J. Chem. Phys.* **1983**, *78*, 6947.
(14) Weiss, J. H. *J. Chem. Phys.* **1984**, *80*, 2880.
(15) Sumi, H.; Marcus, R. A. *J. Chem. Phys.* **1986**, *84*, 4894.
(16) Nadler, W.; Marcus, R. A. *J. Chem. Phys.* **1987**, *86*, 3906.

TABLE I: Calculated Relative Rate Constants k/k_e for $\rho = 1.5$[a]

ϵ	k_e/ω												
	10^{-8}	10^{-7}	10^{-6}	10^{-5}	10^{-4}	10^{-3}	10^{-2}	10^{-1}	10^{0}	10^{1}	10^{2}	10^{3}
5	1.000	1.000	1.000	0.996	0.970	0.847	0.565	0.259	0.818×10^{-1}	0.194×10^{-1}	0.375×10^{-2}	0.629×10^{-3}
10	0.99 (4)	0.984	0.931	0.800	0.584	0.347	0.163	0.609×10^{-1}	0.182×10^{-1}	0.447×10^{-2}	0.931×10^{-3}	0.170×10^{-3}
15	0.88 (1)	0.756	0.572	0.375	0.211	0.101	0.408×10^{-1}	0.141×10^{-1}	0.419×10^{-2}	0.108×10^{-2}	0.242×10^{-3}	0.482×10^{-4}
20	0.54 (7)	0.383	0.236	0.128	0.611×10^{-1}	0.259×10^{-1}	0.969×10^{-2}	0.322×10^{-2}	0.955×10^{-3}	0.253×10^{-3}	0.603×10^{-4}	0.130×10^{-4}
25	0.24 (1)	0.145	0.774×10^{-1}	0.371×10^{-1}	0.161×10^{-1}	0.630×10^{-2}	0.224×10^{-2}	0.727×10^{-3}	0.215×10^{-3}	0.583×10^{-4}	0.145×10^{-4}	0.330×10^{-5}
30	$0.8 (1) \times 10^{-1}$	$0.46 (0) \times 10^{-1}$	0.224×10^{-1}	0.987×10^{-2}	0.400×10^{-2}	0.149×10^{-2}	0.513×10^{-3}	0.163×10^{-3}	0.482×10^{-4}	0.132×10^{-4}	0.337×10^{-5}	0.802×10^{-6}
35	$0.2 (5) \times 10^{-1}$	$0.12 (8) \times 10^{-1}$	$0.59 (5) \times 10^{-2}$	0.249×10^{-2}	0.963×10^{-3}	0.346×10^{-3}	0.116×10^{-3}	0.365×10^{-4}	0.107×10^{-4}	0.297×10^{-5}	0.773×10^{-6}	0.189×10^{-6}
40	$<10^{-2}$	$0.3 (0) \times 10^{-2}$	$0.14 (5) \times 10^{-2}$	$0.60 (2) \times 10^{-3}$	0.227×10^{-3}	0.793×10^{-4}	0.262×10^{-4}	0.813×10^{-5}	0.239×10^{-5}	0.664×10^{-6}	0.175×10^{-6}	0.437×10^{-7}
45	$<10^{-2}$	$<10^{-3}$	$0.3 (1) \times 10^{-3}$	$0.13 (5) \times 10^{-3}$	$0.51 (8) \times 10^{-4}$	0.180×10^{-4}	0.585×10^{-5}	0.181×10^{-5}	0.530×10^{-6}	0.148×10^{-6}	0.394×10^{-7}	0.100×10^{-7}
50	$<10^{-2}$	$<10^{-3}$	$<10^{-4}$	$0.2 (7) \times 10^{-4}$	$0.11 (0) \times 10^{-4}$	$0.39 (7) \times 10^{-5}$	0.130×10^{-5}	0.400×10^{-6}	0.117×10^{-6}	0.329×10^{-7}	0.882×10^{-8}	0.227×10^{-8}

[a] The absolute values of dimensionless constants k/ω were calculated with the accuracy of $\sim 10^{-10}$ (see Appendix B). The figures in parentheses indicate the eleventh decimal place.

3. Rate Constant Calculation Using the Quasi-One-Dimensional Approximation

The solution of eq 6 is represented as an exponential series:

$$P(y,t) = \sum_n P_n(y) \exp(-k_n t) \tag{10}$$

The damping coefficients k_n are the solutions of the following eigenvalue problem:

$$\left[H + \frac{k(z)}{\omega}\right]\varphi_n(z) = \frac{k_n}{\omega}\varphi_n(z) \tag{11}$$

$$z = (\beta\lambda)^{1/2} y$$

The eigenfunctions $\varphi_n(z)$ combined with initial distribution $P(y,0)$ completely determine the quantities $P_n(y)$ in (10). The parameter

$$\omega = \beta\lambda D = \lambda/\eta \tag{12}$$

can be considered as an inverse relaxation time in an effective potential (7). One can treat the operator H as an oscillator Hamiltonian:

$$H = -\frac{d^2}{dz^2} + \frac{1}{4}z^2 - \frac{1}{2} \tag{13}$$

whereas the sink term $k(z)$ can be transformed to

$$\frac{k(z)}{\omega} = \rho^{1/2}\frac{k_e}{\omega}\exp\{-\rho[z - (2\epsilon)^{1/2}]^2 + z^2\} \tag{14}$$

where we took into account relations 7–9 and introduced the parameters

$$\rho = \mu/\lambda, \quad k_e = \frac{\omega_e}{2\pi}\rho^{-1/2}\exp(-\beta U^*)$$

$$\epsilon = \frac{1}{2}(z^*)^2 = \frac{\beta\lambda}{2}(y^*)^2 \tag{15}$$

So we come out with the dimensionless rate constant k/ω as a function of three parameters: k_e/ω, ϵ, and ρ. The quantity k_e coincides with the large friction asymptote of the two-dimensional equilibrium rate constant k (eq 4). According to (12) the ratio k_e/ω is proportional to the medium friction constant. The dimensionless parameter ϵ is associated with a reorganization of the slow variable y, characterizing how sharp the PES relief is along the bottom of the valley $\bar{x}(y)$. Finally, ρ is the ratio of force constants corresponding to the pair of effective potentials $V_1(y)$ and $V(y)$ (eq 7).

If a single-exponential approximation of expansion 10 is accepted, the lowest eigenvalue k_0 becomes a rate constant. As a rule, k_0 proves to be extremely small, which makes its calculation infeasible by standard techniques. The numerical results obtained previously by the moment method[16] fall within a narrow range of parameters (see Figure 5). This range was significantly extended by our calculations performed using the special procedure described in Appendix B. The parameters were studied within the following intervals: $10^{-8} \le k_e/\omega \le 10^3$; $5 \le \epsilon \le 50$; $0.5 \le \rho \le 6.0$. We observed a close agreement with the moment method results[16] in the common parameter range.

Calculations for a typical value $\rho = 1.5$ are listed in Table I. They illustrate the previously predicted[10,11] nonequilibrium kinetic behavior appearing as small values of k/k_e. This type of solution predominates at large ϵ values ($\epsilon \ge 10$) which corresponds either to a sharp PES relief along the medium coordinate or to a low temperature. On the other hand, at small ϵ the ratio k/k_e is close to unity and changes slowly in a large range of k_e/ω, the parameter representing the friction change. This fact allows separation of a pair of different regions in the plane defined by parameters k_e/ω and ϵ as corresponding to equilibrium and nonequilibrium versions of single-exponential kinetics. The corresponding dividing boundary (the solid stepwise line in the upper left corner of Table

I) is drawn conventionally at the level $k/k_e \approx {}^1/_2$. The model estimate of this boundary[10]

$$\frac{k_e}{\omega} = \frac{1}{2\rho^{1/2}}(\epsilon - 1)e^{-\epsilon} \tag{16}$$

shows its exponential dependence on ϵ. The validity of formula 16 in the case $\epsilon \gg 1$ is confirmed by the calculation, as is seen from Table II.

With increasing friction the kinetics at last enters the multiexponential region described by (10). The present calculations were not fit to treat this regime. We were able only to estimate the corresponding boundary by comparing the calculated values of the zeroth (the lowest one) and the first eigenvalue of eq 11: $k_0/k_1 \ll 1$. In the parameter range that we considered, the spectrum of the Hamiltonian (eq 11) retains oscillatory character, the level spacing being approximately ω (see Table III). That is why since $k_0 = k$ we obtain an inequality:

$$k/\omega \ll 1 \tag{17}$$

defining the boundary of the single-exponential kinetic regime. The corresponding stepwise solid line in the upper right corner of Table I is drawn at the level $k/\omega \approx 10^{-1}$. This boundary, contrary to the boundary of eq 16 is very sensitive to variations of the parameter ρ (see Table IV). We were unable to find a satisfactory analytical representation for it.

As data of Table I show, the value of k/k_e can significantly (by 10 orders of magnitude or even more) deviate from unity. The plots of $\ln (k/k_e)$ versus individual parameters k_e/ω, ϵ, and ρ are shown in Figures 1–4. After a parameter reaches some value in the essentially nonequilibrium region, the quantity $\ln (k/k_e)$ varies practically linearly with ϵ and, as a first approximation, linearly with $\ln (k_e/\omega)$. Its dependence on both ϵ and $\ln (k_e/\omega)$ (displaying the increasing degree of nonequilibrium behavior) becomes more sharp the larger the value of ρ. The whole picture agrees with previous qualitative conclusions.[10,11,15,16]

4. Essentially Two-Dimensional Kinetic Regimes

The diffusion-like eq 6 generating the kinetics as described in section 3 was obtained as an extreme case of the original eq 1 when the dynamical vibrational frequency associated with the chemical coordinate x greatly exceeded the characteristic frequency of the medium variable y, which was associated with its relaxation. There exists a range of parameters where the quasi-one-dimensional approximation (6) fails to work properly. The equilibrium kinetics here obeys KGH theory and can be calculated by formulas 4 and 5. The matrices of masses and friction coefficients are

$$\hat{m} = \begin{bmatrix} m & 0 \\ 0 & 0 \end{bmatrix}; \quad \hat{\eta} = \begin{bmatrix} 0 & 0 \\ 0 & \eta \end{bmatrix} \tag{18}$$

whereas the force constant matrices are found by using (3) to be

$$\hat{U}_0 = \begin{bmatrix} \lambda_x + \alpha^2\lambda_y & -\alpha\lambda_y \\ -\alpha\lambda_y & \lambda_y \end{bmatrix}; \quad \det \hat{U}_0 = \lambda_x\lambda_y > 0$$

$$\hat{U}^\ddagger = \begin{bmatrix} \lambda_x^\ddagger + \alpha^2\lambda_y & -\alpha\lambda_y \\ -\alpha\lambda_y & \lambda_y \end{bmatrix}; \quad \det \hat{U}^\ddagger = \lambda_x^\ddagger\lambda_y < 0 \tag{19}$$

$$\lambda_x = \partial^2 U_1/\partial x^2 > 0 \quad \text{(at the reactant minimum)}$$

$$\lambda_x^\ddagger = \partial^2 U_1/\partial x^2 < 0 \quad \text{(at the saddle point)}$$

The decay frequency Ω obtained as a solution of eq 5 in the extreme cases of a small ($\eta \to 0$) and large ($\eta \to \infty$) friction reduces to a simple form:

$$\Omega = (-\lambda_x^\ddagger/m)^{1/2} = \omega_x^\ddagger \quad (\eta \to 0)$$

$$\Omega = (-(\lambda_x^\ddagger + \alpha^2\lambda_y)/m)^{1/2} = \omega_e^\ddagger \quad (\eta \to \infty)$$

TABLE II: Boundary of the Equilibrium Region $(k_e/\omega)(\epsilon)$

	$\rho = 1.5$		$\rho = 6.0$	
ϵ	calcd	formula (eq 16)	calcd	formula (eq 16)
5	10^{-1}–10^{-2}	1.1×10^{-2}	10^{-1}–10^{-2}	5.5×10^{-3}
10	10^{-3}–10^{-4}	1.7×10^{-4}	10^{-3}–10^{-4}	8.3×10^{-5}
15	10^{-5}–10^{-6}	1.7×10^{-6}	10^{-5}–10^{-6}	8.7×10^{-7}
20	10^{-7}–10^{-8}	1.6×10^{-8}	10^{-7}–10^{-8}	8.0×10^{-9}

TABLE III: Lowest Eigenvalues k_0 and k_1 of Eq 11 in Multiexponential Region ($\rho = 1.5$)

k_e/ω	ϵ	k_0/ω	k_1/ω	$(k_1 - k_0)/\omega$
10	5	0.194	1.584	1.390
10	10	0.045	1.210	1.165
10^2	5	0.375	1.942	1.567
10^2	10	0.093	1.356	1.263

TABLE IV: Dependence on ρ of the Boundary of the Polyexponential Region, As Defined by Condition 17

	boundary values k_e/ω		
ϵ	$\rho = 1.5$	$\rho = 3.0$	$\rho = 6.0$
5	10^0	10^1	10^2
10	10^2	$>10^3$	$>10^3$

(Here we accept that $\lambda_x^\ddagger + \alpha^2\lambda_y < 0$ because otherwise the quasi-one-dimensional theory becomes inconsistent; see Appendix A.) The rate constant (4) in the so-indicated limits equals

$$k = (\omega_x/2\pi)\exp(-\beta U^\ddagger); \quad \omega_x = (\lambda_x/m)^{1/2} \quad (\eta \to 0) \tag{20}$$

$$k = \rho^{-1/2}(\omega_e/2\pi)\exp(-\beta U^\ddagger) = k_e \quad (\eta \to \infty) \tag{21}$$

$$\omega_e = \left(\frac{\lambda_x + \alpha^2\lambda_y}{m}\right)^{1/2}; \quad \rho = \mu/\lambda$$

$$\lambda = \frac{\lambda_x\lambda_y}{\lambda_x + \alpha^2\lambda_y}; \quad \mu = \frac{\lambda_x^\ddagger\lambda_y}{\lambda_x^\ddagger + \alpha^2\lambda_y}$$

The limit (20) represents an equilibrium rate constant for the one-dimensional system "a chemical subsystem + instantaneously adjusting medium". Another extreme case (eq 21) obviously coincides with the rate constant k_e (eq 15) arising in the quasi-one-dimensional theory as the equilibrium limit. When the friction η increases, the KGH rate constant (4) varies monotonically between the extremes (20) and (21). This can be proved by analyzing eq 5. The conditions ensuring that limits (20) or (21) are indeed reached are formulated as inequalities for the characteristic medium relaxation frequency $\omega_y = \lambda_y/\eta$. So for the limit (20) we obtain

$$\omega_y \gg \omega_x^\ddagger \tag{22}$$

and for the limit (21)

$$\omega_y \ll \omega_e^\ddagger \tag{23}$$

As is clear from the above discussion, the condition (23) establishes the boundary between essentially two-dimensional kinetic regimes in the equilibrium region. On the other hand, as the calculations of section 3 show, the increase of the parameter ϵ at fixed k_e/ω results in a remarkable breakdown of the equilibrium behavior. This fact definitely indicates that there exists an essentially two-dimensional nonequilibrium kinetic regime, obeying neither eq 4 nor eq 6. It is expected to operate in the region where ϵ is sufficiently large (so that its quasi-one-dimensional counterpart is strongly nonequilibrium) and η (or k_e/ω) is sufficiently small (so that condition (23), ensuring that the process can proceed as a quasi-one-dimensional one, is violated). The location of boundaries separating this new type of solution from the two-dimensional equilibrium region and from the one-dimensional nonequilibrium one depends on many dynamical factors and, in particular, on the shape of the potential $U(x,y)$. So on a PES with

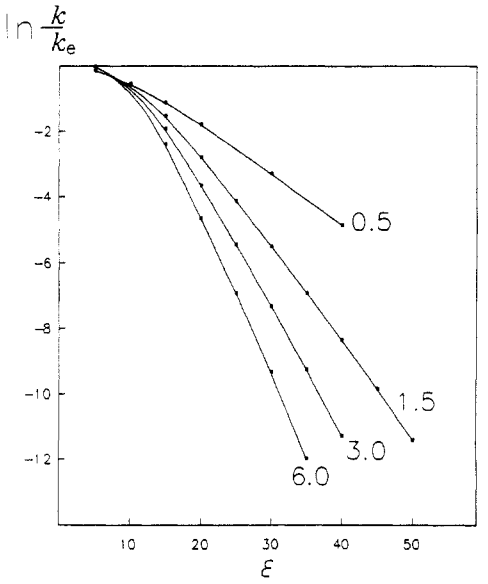

Figure 1. Dependence of ln k/k_e on ϵ for different ρ (figures on the curves) at $k_e/\omega = 10^{-4}$.

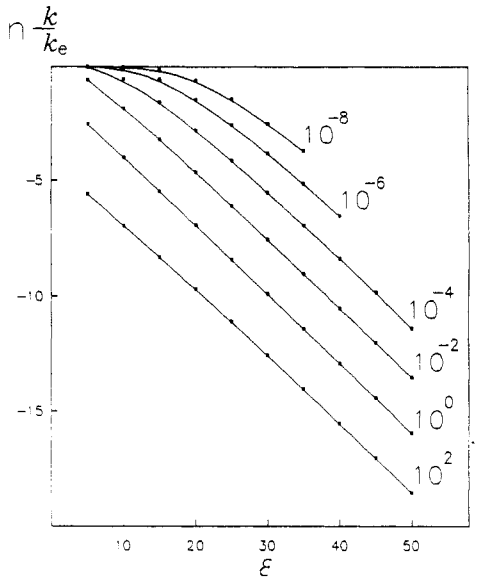

Figure 3. Dependence of ln k/k_e on ϵ for different k_e/ω (figures on the curves) at $\rho = 1.5$.

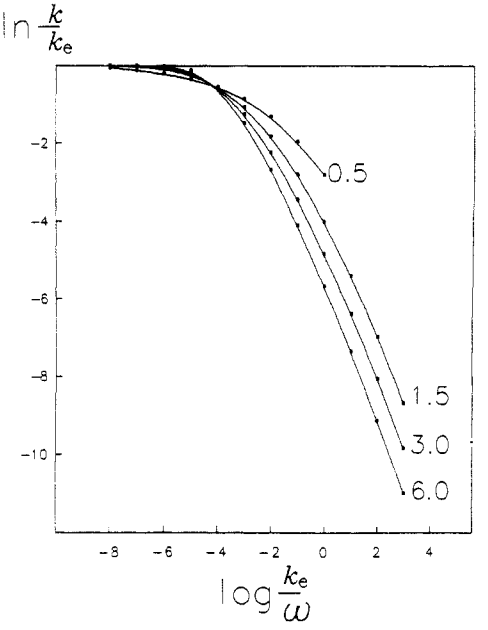

Figure 2. Dependence of ln k/k_e on log k_e/ω for different ρ (figures on the curves) at $\epsilon = 10$.

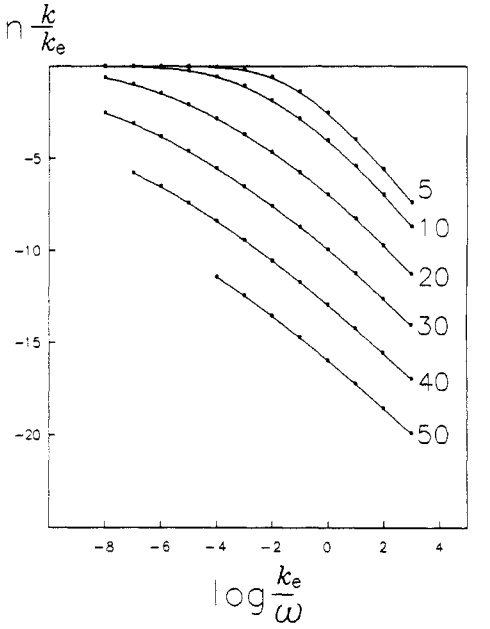

Figure 4. Dependence of ln k/k_e on log k_e/ω for different ϵ (figures on the curves) at $\rho = 1.5$.

complete separation of coordinates x and y the reaction will proceed as an equilibrium at any ratio of characteristic frequencies k_e/ω. Such a situation arises on potential (3) either if $\epsilon \to 0$ or if $\alpha = 0$, that is to say, if $y_0(x) = 0$. When y_0 is x dependent, then the dynamical interaction increases on a sharper PES relief as governed by the increase of parameter ϵ. In general, the boundaries depend in a complicated manner on both the potential parameters and the ratio of characteristic frequencies. A special investigation of this region is needed, on both numerical and model levels, to complete the qualitative kinetic description of model (1).

5. Discussion

Figure 5 summarizes our conclusion as a diagram of kinetic regimes generated by eq 1. The natural parameters of the quasi-one-dimensional approximation, namely, k_e/ω and ϵ, are taken as variables efficiently describing the whole diagram. The diagram borders correspond to the range of parameters within which numerical calculations were available. The region where the kinetics was calculated earlier by the moment method is bounded by the dotted line.

The large parameter range where the kinetics shows a single-exponential form is evident from Figure 5. The multiexponential region (p) is shifted to the upper right corner of the diagram. The large single-exponential region consists of nonequilibrium (n) and equilibrium (e) kinetic subregions. These two are, in turn, subdivided into essentially two-dimensional ($2/n$ and $2/e$) and quasi-one-dimensional ($1/n$ and $1/e$) parts. The farthest to the left one-dimensional equilibrium region $1'/e$ depicts the case of the medium instantaneously adjusting to a slow chemical subsystem. The boundaries of two-dimensional nonequilibrium region $2/n$ (the dashed lines) are shown tentatively because neither calculations nor a qualitative theory are yet available for this region.

The parameters k_e/ω and ϵ are most convenient to treat the quasi-one-dimensional region; however, even here the explicit boundary lines depend on the third parameter ρ. In the two-dimensional region many more parameters influence a kinetic behavior, and the choice of k_e/ω and ϵ as diagram coordinates provides a rather poor representation of the diversity of real kinetics. As a result, the positions of interregion boundaries become less definite. To illustrate this reasoning, it is expedient

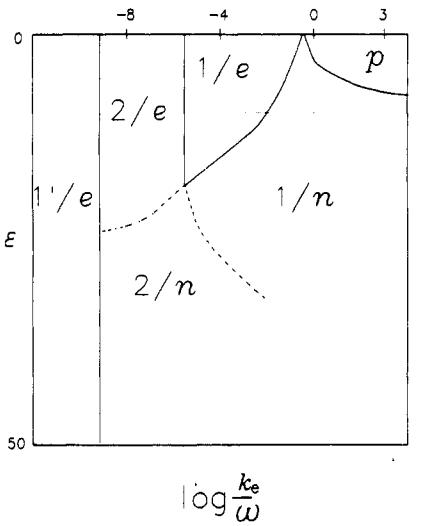

Figure 5. Diagram of kinetic regimes generated by eq 1. The designation of regions: *e*, equilibrium single exponential; *n*, nonequilibrium single exponential; *p*, multiexponential. The numbers indicate an effective dimensionality of the system; 2, essentially two-dimensional; 1, quasi-one-dimensional of the diffusion type; 1', one-dimensional with the instantaneously adjusting medium. The dots indicate the borders of calculations performed by the moment method.[16]

to discuss in more detail the significance of the potential barrier height U^* as a parameter governing the boundaries between different kinetic regimes.

The subregions $1'/e$ and $1/e$ embody two asymptotes of the equilibrium kinetic region e where the KGH rate expression (4) works. The boundaries separating them from the two-dimensional subregion $2/e$ are most conveniently expressed in terms of characteristic frequencies ω_x^*, ω_e^*, and ω_y inherent to the two-dimensional system. So when k_e/ω and ϵ are used as governing parameters, the location of the $(1/e)/(2/e)$ boundary becomes ambiguous because the value $k_e/\omega \sim (\omega_e^*/\omega_y)\exp(-\beta U^*)$ depends sharply on the activation energy U^*. Moreover, the quantity U^*, being a saddle-point energy, bounds ϵ from above by the obvious inequality $\epsilon < \beta U^*$. That is why the activation energy is an important parameter restraining physically accessible limits of parameters k_e/ω and ϵ, although it does not enter the quasi-one-dimensional model explicitly as an essential parameter.

Let us conclude with the notion that the picture shown is true for the PES (2) of a special shape, implying that its cross sections along the medium coordinate are always single-well curves that can be readily approximated as parabolas. This is not true in general. One can imagine a potential displaying double-well cross sections along a medium coordinate in systems with strong interaction. The kinetic behavior changes drastically if such a situation arises within a saddle-point region of a PES or, more generally, in the vicinity of that PES region where most of reactive trajectories are accumulated. This PES structure is typical for reactions in polar solvents when they are accompanied by a large redistribution of electron density and proceed via an electron-transfer mechanism.[6] The kinetic regimes in such systems need special investigation, which proves to be quite easy for a simple model case with a single-well parabolic potential along the chemical coordinate x. We then obtain the same dynamical system (1) with the potential

$$U(x,y) = U_1(y) + \tfrac{1}{2}\lambda_x[x - \alpha y]^2 \qquad (24)$$

taken instead of (3), $U_1(y)$ being a double-well curve. After averaging over the fast variable x, we have the familiar one-dimensional Kramers equation for the slow medium variable in the effective averaged double-well potential. If no mass is associated with the medium motion, as in (1), the result will be the overdamped Kramers rate expression, proportional to η^{-1}. It is remarkable that the same result is obtained after performing the limit $\eta \to \infty$ in the corresponding two-dimensional KGH rate constant (4). Thereby we conclude that for the particular PES surface (24) the KGH treatment seems to work satisfactorily within the whole range of characteristic time scales.

Acknowledgment. We are grateful to Dr. A. M. Berezhkovskii and Dr. V. Yu. Zitserman for interesting discussions.

Appendix A

Specification of the PES (3). Consider the potential (3)

$$U(x,y) = U_1(x) + \tfrac{1}{2}\lambda_y[y - \alpha x]^2 \qquad (A.1)$$

The explicit specification of the potential $U_1(x)$, which allows an exact reduction to the quasi-one-dimensional model of section 3, represents a combination of two parabolas matched at point $x = X$:

$$U_1(x) = \tfrac{1}{2}\lambda_x x^2 \quad (x < X)$$

$$U_1(x) = U^* + \tfrac{1}{2}\lambda_x^*(x - x_b)^2 \quad (x > X) \qquad (A.2)$$

Additionally we assume

$$\lambda_x > 0, \quad \lambda_x^* < 0$$

$$\lambda_b > X > 0 \qquad (A.3)$$

The minimum and maximum of $U_1(x)$ are located at $x = 0$ and $x = x_b$, respectively. The second (product) minimum is absent in this model. The matching point X is the root of the equation

$$\tfrac{1}{2}\lambda_x X^2 = U^* + \tfrac{1}{2}\lambda_x^*(X - x_b)^2 \qquad (A.4)$$

The reactant minimum and the saddle point of PES, (A.1) and (A.2), correspond to the points

$$x_0 = 0, \quad y_0 = 0 \quad \text{(minimum)}$$

$$x^* = x_b, \quad y^* = \alpha x_b \quad \text{(saddle point)} \qquad (A.5)$$

Next we obtain a pair of lines satisfying the condition $\partial/\partial x\,[U(x,y)] = 0$. They are defined by the expressions

$$\bar{x} = \frac{\alpha\lambda_y}{\lambda_x + \alpha^2\lambda_y} y; \quad \bar{x} < X \qquad (A.6)$$

(the line of minima or the valley) and

$$\bar{x}^* = x_b + \frac{\alpha\lambda_y}{\lambda_x^* + \alpha^2\lambda_y}(y - \alpha x_b); \; \bar{x}^* > X \qquad (A.7)$$

(the line of maxima or the ridge). The PES cross sections along these lines are calculated to be

$$V(y) = U(\bar{x},y) = \frac{1}{2}\frac{\lambda_x\lambda_y}{\lambda_x + \alpha^2\lambda_y} y^2$$

$$V_1(y) = U(\bar{x}^*,y) = U^* + \frac{1}{2}\frac{\lambda_x^*\lambda_y}{\lambda_x^* + \alpha^2\lambda_y}(y - \alpha x_b)^2 \qquad (A.8)$$

The theory of section 3 works under the condition

$$\lambda_x^* + \alpha^2\lambda_y < 0 \qquad (A.9)$$

which ensures that all PES cross sections along x have maxima at points $\bar{x}^*(y)$. There exists an additional limitation following from (A.6):

$$\bar{x}(y=y^*) = \frac{\alpha^2\lambda_y}{\lambda_x + \alpha^2\lambda_y} x_b < X \qquad (A.10)$$

Together with (A.4) it confines the choice of parameters of the potential (A.1) and (A.2).

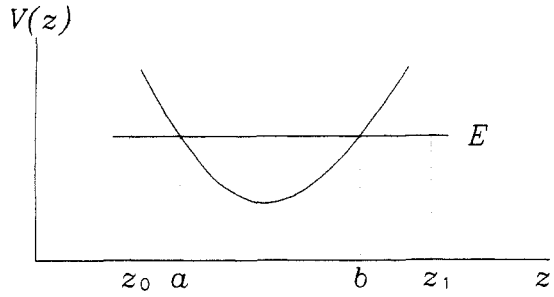

Figure 6. Calculation of eigenvalues of operator (11).

Appendix B

Calculation of Eigenvalues of Eq 11. Our method is based on the statement that the eigenvalues of the Schroedinger equation are zeroes of the corresponding Jost function.[17] It was applied earlier to calculate resonance states in a multichannel scattering problem[18] and also when studying tunneling effects in a one-dimensional double-well potential with five turning points.[19] The method enables one to detect small corrections to the unperturbed energy level even if a perturbation operates in a classically inaccessible region of a potential. This is an important advantage over standard prescriptions based on the diagonalization of a Hamiltonian matrix in a finite size truncated basis set.

The Jost function W_σ corresponding to eq 11, which is reduced after obvious redesignations to a familiar Schroedinger form

$$\left[-\frac{\hbar^2}{2m}\frac{d^2}{dz^2} + V(z)\right]\varphi(z) = E\varphi(z) \qquad (B.1)$$

is defined as a Wronskian composed of two solutions. These are $\sigma(z)$, the asymptotic solution in the classically inaccessible region (Figure 6) and the regular solution $\varphi(z)$, both corresponding to energy E:

$$W_\sigma(E) = W[\sigma(z|E), \varphi(z|E)] \qquad (B.2)$$

The Wronskian (B.2) is calculated at point z_1 located in the asymptotic region where

$$\sigma(z_1) = \mathcal{H}(z_1)^{-1/2}\exp(-w_1) \qquad (B.3)$$

$$w_1 = \int_b^{z_1}\mathcal{H}(z)\,dz, \quad \mathcal{H} = (1/\hbar)(2m[V(z) - E])^{1/2}$$

The regular solution at z_1 can be found by a calculation of the propagator **R** connecting solutions of eq B.1 and their derivatives in two asymptotic regions:

$$\begin{bmatrix}\varphi(z_1)\\ \varphi'(z_1)\end{bmatrix} = \mathbf{R}(z_1,z_0)\begin{bmatrix}\sigma(z_0)\\ \sigma'(z_0)\end{bmatrix}; \quad \mathbf{R} \equiv \begin{bmatrix}r_1 & r_2\\ r_3 & r_4\end{bmatrix} \qquad (B.4)$$

We calculated the Wronskian and obtained the following equation for eigenvalues of (B.1):

$$\frac{1}{(\mathcal{H}_0\mathcal{H}_1)^{1/2}}r_3 + \left(\frac{\mathcal{H}_0}{\mathcal{H}_1}\right)^{1/2}r_4 + \left(\frac{\mathcal{H}_1}{\mathcal{H}_0}\right)^{1/2}r_1 + (\mathcal{H}_0\mathcal{H}_1)^{1/2}r_2 = 0 \qquad (B.5)$$

The matrix **R** is available by a standard numerical integration of eq B.1 between classically inaccessible points z_0 and z_1, which are implied to be sufficiently well separated from the respective turning points. Specifically, their positions were selected to satisfy the condition

$$w \geq 10$$

imposed on a quasiclassical phase integral

$$w = 1/\hbar\int(2m[V(z) - E])^{1/2}\,dz$$

The integration limits were (z_0,a) and (b,z_1). Then the quasiclassical wave functions at z_0 and z_1 are $\mathcal{H}^{-1/2}\exp(-w) \leq 10^{-5}$, which ensures an absolute accuracy of the eigenvalue calculations to be no worse than 2×10^{-10} times the value of the vibrational quantum corresponding to the potential $V(z)$.

(17) Newton, R. C. *Scattering Theory of Waves and Particles*; McGraw-Hill: New York, 1966.
(18) Basilevsky, M. V.; Ryaboy, V. M. *Chem. Phys.* **1984**, *86*, 67.
(19) Basilevsky, M. V.; Ryaboy, V. M. *Mol. Phys.* **1981**, *44*, 785.